Desalination and Water Treatment
www.deswater.com

doi: 10.1080/19443994.2015.1112311

57 (2016) 20944–20956
September

Taylor & Francis
Taylor & Francis Group

Enhanced arsenic removal from drinking water by iron-enriched aluminosilicate adsorbent prepared from fly ash

Alok Kumar Meher[a], Sera Das[b], Sadhana Rayalu[a], Amit Bansiwal[a,*]

[a]*Environmental Materials Division, National Environmental Engineering Research Institute, Nehru Marg, Nagpur 440020, India, emails: ak_meher@neeri.res.in (A.K. Meher), s_rayalu@neeri.res.in (S. Rayalu), Tel./Fax: +91 71272247828; email: ak_bansiwal@neeri.res.in (A. Bansiwal)*

[b]*Analytical Instrumentation Division, National Environmental Engineering Research Institute (Council of Scientific and Industrial Research), Nehru Marg, Nagpur 440020, India, email: s_das@neeri.res.in*

Received 24 April 2015; Accepted 17 October 2015

ABSTRACT

The study deals with an efficient approach for the utilization of fly ash and mitigating one of the most severe drinking water problems caused due to arsenate. Iron enriched aluminosilicate adsorbent (IEASA) was synthesized using a novel method of alkali fusion of fly ash followed by ageing and hydrothermal curing. The raw material, intermediates, and final products were thoroughly characterized using powder X-ray diffraction, Fourier transform infrared spectroscopy, scanning electron microscopy, and particle size analysis. The characterization results suggested that the prepared adsorbent is highly crystalline with particle size of <500 nm. The IEASA was evaluated as an adsorbent for the removal of arsenate at initial concentration of 1 mg L^{-1} by batch adsorption studies, which shows excellent removal efficiency for arsenate (above 99%) in wide pH range of 4–10 and in the presence of various interfering ions. The efficiency was also compared with synthetic zeolite, which shows negligible arsenate removal. Adsorption isotherms were plotted using the Langmuir and Freundlich models to compute the adsorption capacities. The adsorption capacity obtained from Langmuir isotherm was 0.592 mg g^{-1} as compared to the adsorption capacity of 0.455 mg g^{-1} calculated from kinetics data. Detailed kinetics studies were also carried which confirms that the adsorption kinetics follows pseudo-second-order and particle diffusion is the rate determining step. Water quality was evaluated before and after adsorption, which suggests the suitability of the adsorbent for the decontamination of arsenate from drinking water and other parameters also confirms that treated water is potable.

Keywords: Aluminosilicate adsorbent; Arsenate; Drinking water

1. Introduction

The occurrence of arsenic in natural water is a worldwide problem. Globally, over 130 million people are estimated to be potentially exposed to arsenate in drinking water at concentrations above the World Health Organization (WHO) guideline value of 10 μg L^{-1} and the number is likely to grow. Arsenic contamination of Indo-Gangatic planes (India and Bangladesh) is considered as one of the biggest natural calamity due to geogenic contaminants. Anthropogenic sources of arsenic include industrial effluents

*Corresponding author.

from metallic alloys, paint manufacturing, fireworks, glass manufacturing, and electrical semiconductors. Arsenic is also used extensively in the production of agricultural pesticides, including herbicides, insecticides, desiccants, wood preservatives, and feed additives [1].

The International Agency for Research on Cancer (IARC) classified arsenic, a toxic metalloid, as a Group 1 carcinogen [2]. Exposure to high concentration of arsenic leads to kidney, lung, bladder, liver, and skin cancer [3–7]. Because of the toxicological effects of arsenic, the guideline value in drinking water is set as low as 10.0 μg L^{-1} as per authorities like Bureau of Indian Standards in 2012 [8], WHO in 2011 [9], European Union in 2014 [10], and United States Environmental Protection Agency in 2009 [11].

Arsenic removal from ground water is a challenging task due to large variation in physiochemical forms at different conditions. The major arsenic removal technologies includes oxidation, precipitation/coprecipitation, coagulation, sorption, ion exchange, and reverse osmosis [12–15]. Although these methods have been widely employed, they have several drawbacks like high operating and waste treatment costs, high consumption of reagents and large volume of sludge formation.

Adsorption methods are considered to be most effective method for water treatment because of their treatment efficiency, ease of operation, and compact unit processes owing to which technology is universally acceptable and commercially available. It is particularly well accepted by the rural people of developing countries because of simple operation, low cost, and a potential for regeneration and sludge free operation. Moreover, among various water treatment technologies, adsorption is relatively fast, inexpensive and provides a flexible option of regeneration of saturated adsorbent. Adsorbents such as carbon and activated alumina are well known for the treatment of drinking water [16,17].

There is growing interest in using low-cost materials to remove arsenic from water. Many biological derivatives (bio char, chitin, chitosan, cellulose sponge, some biomass, biogenic manganese oxides mineral), oxides (clay, manganese oxide, activated alumina, titanium dioxide, aluminum hydroxide, lanthanum hydroxide, ferrihydrite/iron hydroxide/iron oxides, zirconium oxide, mixed rare earth oxides, hydrotalcites, etc.), industrial wastes (rice husk, red mud, calcined bauxite), and polymer resins (Amberlite IRC-718, Dowex 2N, PolyHIPE, LEWATIT TP 207, amberlite XAD-7, bayoxide E33, arsenex) are well reported for adsorbents of arsenate [17–22].

Several researchers have reported removal of arsenate and arsenite by different types of aluminosilicate materials, like clinoptilolite, chabazaite, SZP1, 13X, and 5A [22–30]. In order to improve the affinity toward arsenic several modified Zeolites have also been reported such as iron-exchanged natural zeolites [31–40], MnO_2-modified zeolite [41]. It has been reported that terminal aluminol or silanol hydroxyl groups present at the edges of the zeolite particle can be easily replaced by arsenic [42]. Surfactant-modified zeolites have also reported as potential adsorbent for arsenic [43–49].

In the present work, studies are focused on evaluation of the effectiveness of the iron-enriched aluminosilicate adsorbent (IEASA) prepared from fly ash for arsenate removal from aqueous solution. Zeolites are hydrated crystalline alumina silicates with uniform pore size, reversible hydration, and ion exchanging, sportive and sieving ability that make them potentially useful as adsorption mineral for use in the ground waters. Properties of zeolites vary with Si/Al ratio. When the Si/Al is around 1, the type of Zeolite is termed as Zeolite-A. There are many advantages of using zeolites or aluminosilicates as an adsorbent for arsenate removal, over others namely high capability of removing arsenate species in the form of both arsenate and arsenite from an aqueous medium, effective in wide range of pH value and in the presence of coions like Cl^-, PO_4^-, SO_4^-, NO_3^-, HCO_3^-, and CO_3^-.

The objective of the present study was to study the efficacy of IEASA for the removal of arsenate. Other objectives include study of properties of IEASA as a function of several factors namely dose of the adsorbent and effect of pH. Kinetics study has also been performed in order to predict the rate of reaction. Efficiency of the adsorbent has also been evaluated in presence of other coions, which are commonly present in water.

2. Materials and methods

2.1. Materials

Fly ash used for the preparation of IEASA was collected from ash dyke of coal-based power plant located at Tanda, U.P., India. Elemental analysis confirms that the fly ash was of F-grade, according to ASTM C618 standards. The material was used as such after sieving with 70 micron sieve followed by washing with deionized (DI) water (18 MΩ resistivity, obtained from MilliQ DI water system). Sodium hydroxide, sodium arsenate, and sodium aluminate were purchased from E. Merck India Ltd. A stock

solution of 1,000 mg L^{-1} arsenate was prepared by dissolving 4.1631 g of di-sodium hydrogen arsenate heptahydrate in 1,000 ml of DI water and working solutions of different arsenate concentrations were prepared freshly by appropriate dilution of stock solution by DI water. All chemicals used in this study were of analytical grade.

2.1.1. Material synthesis

(1) Iron-enriched aluminosilicate adsorbent (IEASA)

The IEASA was synthesized using a novel and patented process developed by our group. IEASA was prepared by following this process except for one change wherein the step of magnetic separation of iron was intentionally omitted to retain the iron present in the fly ash. Briefly, the process is as follows:

The raw fly ash (RFA) samples were first screened through a sieve of 70 μm-mesh size to eliminate the coarser particles. The fly ash was then washed and dried followed by calcination at 800˚C for 2 h to remove the unburnt carbon and volatile materials. The fly ash samples were subjected to fusion with sodium hydroxide in a ratio of 1:1.2 in a muffle furnace at temperature of 580˚C for 1.5 h. A homogeneous fusion mixture was obtained by grinding. The resultant fused mass was mixed thoroughly in distilled water with simultaneous addition of sodium aluminate. The slurry so obtained was then subjected to stirring at room temperature for 12 h. The resulting slurry was then subjected to hydrothermal crystallization in a closed Teflon vessel at 100˚C for definite time duration. The final product was washed thoroughly to remove excess alkali and dried at 100˚C for 12 h.

(2) Commercial aluminosilicate adsorbent (CZA) used for competitive studies was procured from MEHA Chemicals, India.

2.1.2. Characterization of the adsorbent

Elemental analysis was done to determine the chemical composition of the fly ash and IEASA. The elemental composition of fly ash and aluminosilicate material was determined by microwave acid digestion method. About 20 mg of the sample was taken and 5 ml hydrofluoric acid was added followed by 10 ml of aqua regia mixture and 2 ml perchloric acid. The program for complete acid digestion of sample was optimized and found to be 40% power rating for 10 min, 80% power rating for 10 min and 100% power rating for 5 min. After cooling, the solution was mixed with 10 ml of boric acid. The solution was stored and diluted 10 times. Various elements were analyzed in the digested solution using ICP-OES. (Model: iCAP 6000 Thermo scientific).

Powder X-ray diffraction (PXRD) was done to determine the different phases of silica, alumina, zeolites, and other metal oxides. The PXRD patterns were recorded using benchtop X-ray diffractometer (Model: Rigaku Miniflex). The operating target voltage was 30 kV and the current was 15 mA. The radiations of Cu Kα were generated using X-ray generator and the β radiations were suppressed using Ni filter. The sample was powdered and scanned for 2θ ranges from 5˚ to 80˚, with goniometer specification radius of 150 mm and soller slit ±2.5˚ (divergence angle).

Fourier transform infrared spectroscopy (FTIR) spectra were done using instrument made by Bruker, Germany (Model Vertex-70). Spectral study has been done in the range of 400 cm^{-1} to 4,000 cm^{-1} using Drift method with resolutions of 4 cm^{-1} and 16 scans. The detector of the instrument is of DLaTGS type with KBr beam splitter.

The SEM micrographs were obtained using Jeol SEM (Model: JXA-840A) instrument. Carbon coating over the dried sample was done up to thickness 20 nm, since the samples were nonconductive. The working potential difference was maintained at 15 and 20 kV at vacuum depending upon the sample. Working distance was adjusted at 13 mm. Micrographs were obtained at different magnifications.

2.2. Method

2.2.1. Batch adsorption and kinetics studies

The adsorption isotherms were studied by varying dose of adsorbent under a fixed concentration of arsenate at 1 mg L^{-1} and pH at 7.1 ± 0.2. About 100 ml working solution of arsenate was added separately to conical flasks. Replicas were taken for better accuracy. The flasks were kept on laboratory orbital shaker (Maker: Remi) for 8 h at constant temperature of 27 ± 2˚C. The solution was then filtered with Whatman filter paper 42. Filtrate was collected and stored for analysis by adding nitric acid. The amount of arsenate adsorbed was calculated from following equation [50]:

$$q_e = (C_0 - C_e)\frac{V}{w} \quad (1)$$

where q_e is the adsorption capacity (mg g^{-1}) at equilibrium, C_0 and C_e are the initial and equilibrium liquid-phase concentrations of arsenate (mg L^{-1}),

respectively, V is the volume of solution (L) and W is the mass (g) of adsorbent used.

2.2.1.1. pH study. The effect of pH on the adsorption efficiency of material was evaluated by varying the pH of solution from 2 to 10 by the addition of 0.1 N HCl and 0.1 N NaOH.

2.2.1.2. Competitive ion study. Tap water (TW) spiked with 1 mg L^{-1} of arsenate (TW) and simulated water (SW) with the composition of chloride 100 mg L^{-1}, carbonate 200 mg L^{-1}, bicarbonate 50 mg L^{-1}, sulfate 20 mg L^{-1}, and phosphate 1 mg L^{-1} was taken and batch adsorption studies were conducted to evaluate the effect of the presence of coions.

2.2.1.3. Kinetics study. Required quantity of adsorbent was taken in 500 ml of arsenate solution and placed in orbital shaker (Maker: Remi) at a speed of 150 rpm. Samples were taken at predetermined intervals and contents were filtered by syringe filters and residual arsenate concentrations were determined in the filtrate.

2.2.2. Arsenic analysis

Arsenic was analyzed in the acid preserved samples using Inductively Coupled Plasma-Optical Emission Spectrometer (ICP-OES, Model iCAP 6000 Thermo scientific). For the preparation of calibration standards, commercially available (Sigma-Aldrich) arsenic standard stock solution of 1,000 mg L^{-1} was used. Working standard solutions were prepared in the range of 0.01–1.0 mg L^{-1} and the calibration was performed until the correlation coefficient of 0.9999 was obtained.

3. Results and discussion

3.1. Characterization of RFA, CZA, and IEASA

Chemical composition of RFA, CZA, and IEASA are presented in Table 1. It was found that RFA contains 52.42% silica, 30.96% alumina, 5.63% iron oxide, and some other trace elements. Si/Al ratio was almost constant and varies around 1.1 for IEASA and CZA. Constituents like B, CaO, oxides of Na, Mg, and K were also present in same quantity in both the materials. IEASA contains 6.76% iron oxide and CZA shows negligible iron oxide of 0.1%. Besides this IEASA contains slightly elevated level of other elements as compared to CZA. The elemental analysis suggests that IEASA is having a higher iron composition as compared to CZA, which may lead to enhanced arsenate adsorption capacity.

The PXRD patterns of RFA, CZA, and IEASA are presented in Fig. 1. It is evident from results that the major crystalline components in fly ash are of silica (Quartz) and alumina (Mullite) along with some iron oxides and lime. The amorphous aluminosilicate materials may be of glassy phase. Besides, some peaks of iron oxides and lime are also seen. Conversion of fly ash into IEASA results into significant increase in crystalline. On comparison of PXRD patterns of IEASA and CZA, it was found that IEASA has high degree of crystallinity even better than the commercial Zeolites. From the PXRD data, it was also found that the major components include phases of silica and alumina and the amount of amorphous aluminosilicate phases are very less. The values of 2θ, d-spacing and relative intensity $[I/I_0]$ of RFA, CZA, and IEASA are also presented in Table 2. The presence of similar peaks at 2θ angle of 23.9°, 27°, 29.9°, and 34.1° confirms the structural similarity between CZA and IEASA.

Table 1
Elemental composition of RFA, CZA, and IEASA

Material	RFA	CZA	IEASA
SiO_2 (in %)	52.42	48.65	44.72
Al_2O_3 (in %)	30.96	47.37	44.64
Fe_2O_3 (in %)	5.63	0.1	6.76
CaO (in %)	2.85	1.79	2.61
B (in %)	3.66	1.27	3.05
Oxides of Na, K, and Mg (in%)	2.03	0.52	1.43
Trace elements (in %) (As, Ba, Cd, Cr, Ga, Li, Mn, Pb, Se, Sr, Te, Zn)	0.26	0.04	0.3

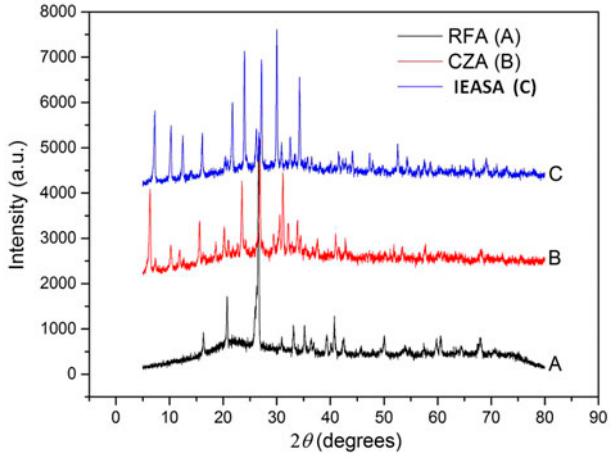

Fig. 1. PXRD patterns of RFA, CZA, and IEASA.

Table 2
PXRD parameters for RFA, CZA, and IEASA

2θ			d-Spacing			I/I_0		
RFA	CZA	IEASA	RFA	CZA	IEASA	RFA	CZA	IEASA
20.78	7.14	7.08	4.721	12.37	12.475	32	41	52
26.66	10.16	10.1	3.341	8.699	8.751	100	35	43
40.72	21.64	21.6	2.214	4.103	4.111	22	56	55
40.82	23.9	23.9	2.209	3.72	3.72	20	91	89
	27.06	27.0		3.30	3.30		60	85
	29.92	29.92		2.984	2.984		100	100
	34.16	31.16		2.623	2.623		68	63

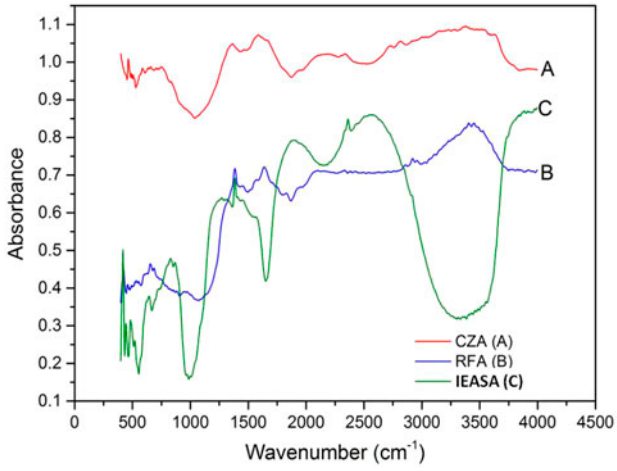

Fig. 2. FTIR spectra of RFA, CZA, and IEASA.

FTIR spectra of RFA, CZA, and IEASA are presented in Fig. 2. FTIR spectra of RFA shows band at 1,020 cm^{-1} which may be assigned to (Si–O–Si) asymmetric stretching vibration. Bands observed at 989.3 and 468.72 cm^{-1} which may be assigned to (Si–O–Si). The FTIR spectra of CZA and IEASA show a number of similar peaks. Peaks observed at 454.73, 498.55, 547.88, can be assigned to asymmetric stretching vibration and T–O bending vibration. The bands at 609.92, 722.59, 978.0, 1,356.02, 1,476.52, 1,602.14, 2,831.92, 3,548.98, and 3,731.03 cm^{-1}, can be assigned to various vibrations of silica and alumina tetrahedra. Band at 454.73 cm^{-1} may be due to the structure insensitive internal TO_4 [T = Si or Al] tetrahedral bending. Band of 498.55 cm^{-1} due to symmetrical stretching vibration in the framework structure. Band of 722.59 cm^{-1} suggests asymmetrical stretching vibration in the framework structure. Band at 609.72 cm^{-1} suggests the presence of T–O band as external linkages. Bridging –OH groups exhibiting additional electrostatic interactions to adjacent oxygens are indicated by band at 3,548.98 cm^{-1}. Attachment of –OH group to multivalent cations like Fe, can be interpreted by band formation at 3,414.98 cm^{-1}, which compensate the negative charge of Si–O–Al framework [51].

The SEM micrographs of RFA, CZA, and IEASA are presented in Fig. 3. It may be interpreted from SEM micrographs that the sizes of the fly ash particles observed in this study ranged from less than 1 to 100 μm and consisted of solid spheres. Hollow cenospheres and irregularly shaped unburned carbon particles were also found in the upper end of the size distribution. Agglomerated particles and irregularly shaped amorphous particles may have been due to inter-particle contact or rapid cooling. Scanning electron microscopy (SEM) study also supports the crystalline nature of IEASA. Clear crystals of cubical shape may be observed of IEASA, which are similar to CZA. The size of the crystals is less than 500 nm for IEASA. The SEM micrographs of IEASA also show agglomerates which are formed due to fine particle size of IEASA.

3.2. Batch adsorption studies

A batch adsorption study was done by taking the initial concentration of arsenate as 1 mg L^{-1} and varying the dose from 0.2 to 4 g L^{-1}. CZA shows the removal efficiency of 32.65% at a dose of 4.0 g L^{-1}, whereas IEASA shows 99.26% removal at the same dose (Fig. 4). Considering the higher removal efficiency of IEASA, detailed adsorption studies were conducted using IEASA.

Various adsorption parameters were obtained by plotting Langmuir and Freundlich isotherm models, to get an insight into the adsorption mechanism. Langmuir isotherm equation is derived from simple mass kinetics, assuming chemisorptions. This model is based on assumptions that no lateral interaction among the molecules and the adsorbed molecule remained at the

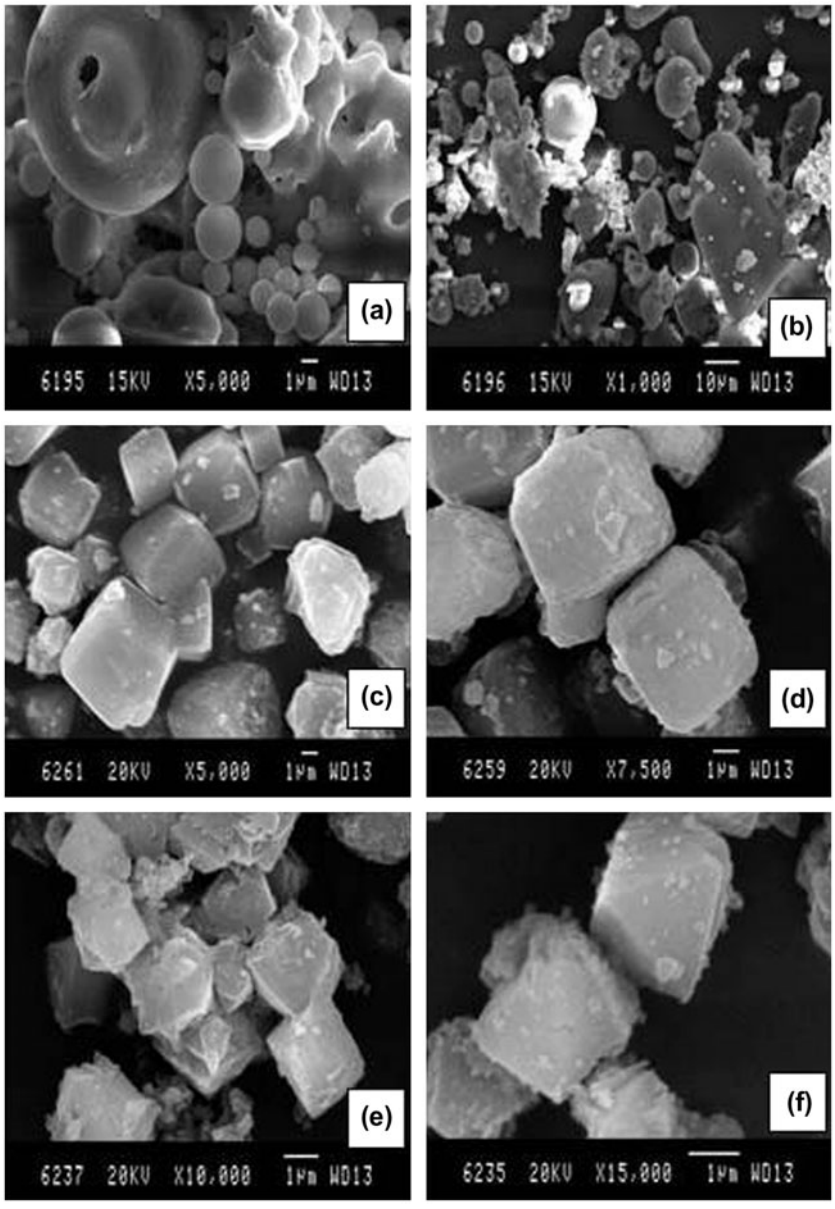

Fig. 3. SEM micrographs of RFA (a and b), CZA (c and d), and IEASA (e and f) at various magnifications.

site of adsorption until it desorbed. Langmuir model is based on monolayer adsorption on uniform, homogeneous surface with sites of identical nature. The linear form can be represented as follows [52]:

$$\frac{1}{q_e} = \frac{1}{q_m K_L C_e} + \frac{1}{q_e} \tag{2}$$

The Freundlich model is based on multilayer adsorption on the heterogeneous adsorbent surface with non-identical sites. The linear form of the Freundlich adsorption model may be expressed as follows [53]:

$$\log(q_e) = \log k + \frac{1}{n}\log(C_e) \tag{3}$$

where q_e is the amount of adsorbate adsorbed per unit weight of the adsorbent at equilibrium (mg g^{-1}), q_m is the maximum adsorption capacity (mg g^{-1}), K_L is the Langmuir constant, C_e is the equilibrium concentration of the adsorbate in solution (mg L^{-1}), K_F is the Freundlich constant, n is the Freundlich constant, which reflects adsorption intensity.

The results of the experimental data were fitted to the linear forms of both the isotherms to determine

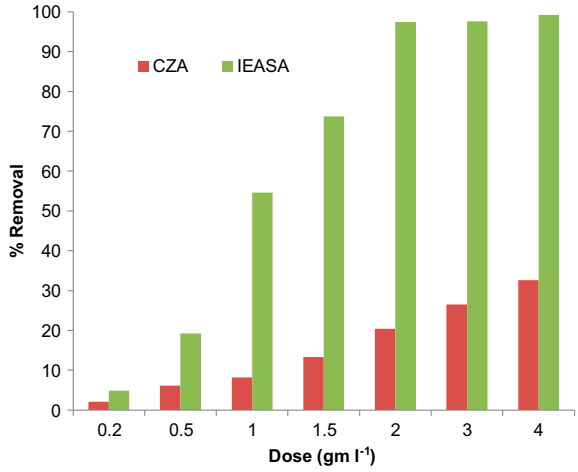

Fig. 4. Comparison of removal efficiency of CZA and IEASA.

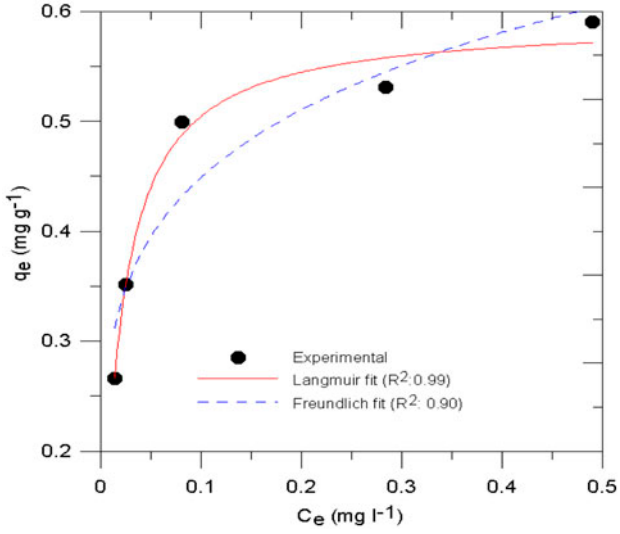

Fig. 5. Langmuir isotherm and Freundlich isotherm for IEASA (batch volume: 100 ml, temperature: 30 ± 2°C, initial As concentation: 1 mg L^{-1}, contact time: 6 h).

Table 3
Parameters of Langmuir and Freundlich model for arsenic adsorption onto IEASA

Langmuir		Freundlich	
q_{max}	0.592	K_F	0.866
b	57.261	$1/n$	0.208
r	0.016	n	4.812
R^2	0.995	R^2	0.903

the best fit model which most accurately described adsorption by the adsorbent. The Langmuir and Freundlich adsorption isotherms for IEASA are presented in Fig. 5. The results of various adsorption parameters obtained from these isotherm models are also presented in Table 3. From the comparison of the fitness between the two isotherms, it is evident that the experimental data for the adsorbents were more well fitted to the Langmuir model compared to Freundlich model, which signify the monolayer adsorption of arsenate on uniform surface. The adsorption capacity for IEASA was found to be distinctly higher than CZA. The calculated adsorption capacity for IEASA obtained from the Langmuir model was found to be 0.592 mg g^{-1}.

3.3. Adsorption kinetics

The kinetics of the arsenate adsorption on IEASA was determined using reaction-based models and diffusion based models and to determine the rate limiting step. In order to study the reaction kinetics, pseudo-first-order and pseudo-second-order models have been used. A linear form of pseudo-first-order kinetic model also known as Lagergren equation is represented as [54]:

$$\ln(q_e - q_t) = \ln q_e - K_{ad}t \quad (4)$$

where q_t is the amount of arsenate adsorbed at time t (mg g^{-1}) and k_{ad} is the equilibrium rate constant of pseudo-first-order adsorption (min^{-1}). The linearized plots of $\log(q_e - q_t)$ vs. t will give the rate constants. The pseudo-second-order model is also used to predict the kinetic parameters, which linear equation can be written as [55]:

$$\frac{t}{q_e} = \frac{1}{h} + \frac{t}{q_e} \quad (5)$$

and

$$h = kq_e^2 \quad (6)$$

where q_t is the amount of arsenate adsorbed at time t (mg g^{-1}), q_e is the amount of arsenate adsorbed at equilibrium (mg g^{-1}), h is the initial sorption rate (mg g^{-1} min^{-1}). The values of q_e (1/slope), k (slope^2/intercept), and h (1/intercept) can be calculated from the plots of t/q_t vs. t.

The linear plots of pseudo-first-order and pseudo-second-order models are presented in Fig. 6. The values of k_{ad}, k, and h and correlation coefficients obtained from the linear plots are also presented in Table 4. It was observed from the values of correlation coefficients that fitness of the pseudo-second-order model is better as compared to pseudo-first-order model. The adsorption capacity calculated from the

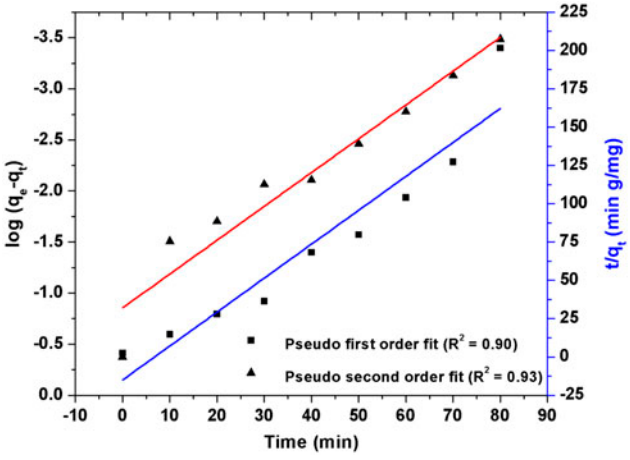

Fig. 6. Pseudo-first-order and pseudo-second-order plots for arsenic adsorption by IEASA (volume: 500 ml, temperature: 30 ± 2°C, initial As concentation: 1 mg L^{-1}, adsorbent dose: 2.5 g L^{-1}).

pseudo-second-order model was 0.455 mg g^{-1}, whereas the adsorption capacity obtained from Langmuir adsorption isotherm was 0.592 mg g^{-1}, which are in close agreement with each other.

Sorption of a liquid adsorbate on porous solid adsorbent can also be modeled by pore diffusion models, which can be either particle diffusion or pore diffusion model. The particle diffusion model can be represented as [56]:

$$\ln\left(\frac{C_t}{C_e}\right) = -k_p t \tag{7}$$

where k_p is the particle diffusion coefficient (mg g^{-1} min). The value of k_p can be obtained by slope of the plot between $\ln(C_t/C_e)$ and t.

The intraparticle pore diffusion model or the Weber and Morris plot is also commonly used to characterize the sorption data. According to this model, if the rate-limiting step is the diffusion of adsorbate within the pores of adsorbent particle (intraparticle diffusion), a graph between the amount of adsorbate adsorbed and square root of time should give a straight line passing through the origin. (Weber and Morris, 1963). The equation can be written as [56]:

$$q_t = k_i t^{0.5} + C \tag{8}$$

where k_i is the intraparticle diffusion coefficient (mg g^{-1} $min^{0.5}$), which can be obtained from the slope of plot of q_t verses $t^{1/2}$ and C is the y intercept of the plot. The plots of linear forms of particle diffusion and intraparticle pore diffusion models are given in Figs. 7 and 8 respectively, and the values of different parameters are given in Table 4. The values of R^2 for particle diffusion model are closer to unity indicating that particle diffusion of absorbent is contributing more towards the rate determining step. The final product (IEASA) is highly crystalline in nature as evident from the XRD patterns and SEM micrographs, even more crystalline than commercial zeolite. It is reported that the sorption of various species in crystalline porous adsorbents follow particle diffusion model, since mass transfer between the particles are the rate determining steps and once the adsorbate reaches the particle surface the intra particle diffusion is fast owing to the highly porous nature of crystalline porous adsorbents. Therefore, it was inferred that the diffusion of adsorbate between the particles plays a significant role in controlling the kinetics of sorption of arsenic on IEASA.

3.4. Effect of pH

Removal of arsenate from water is highly dependent on pH and it has been observed that for most of the adsorbent adsorption capacity reduces with increasing pH. Effect of pH on arsenate removal by aluminosilicate materials has been reported by Elizalde-Gonz´alez et al. [57,58]. pH of the arsenate contaminated ground water is normally reported between 7 and 8.5 and there is a drastic reduction in the uptake capacity of most of the adsorbents between this pH [58,59]. To study the effect of pH on arsenate adsorption capacity of IEASA, arsenate removal was studied at pH ranging between 2 and 10. Initial concentration of the arsenate solution was taken around 1 mg L^{-1} and adsorbent dose was taken 2.5 g L^{-1}. As evident from Fig. 9 there is only slight variation in the efficiency of arsenate removal with variation in pH,

Table 4
Kinetics and diffusion parameters for arsenic adsorption onto IEASA

Pseudo-first-order		Pseudo-second-order			Particle diffusion		Intraparticle pore diffusion		
k_{ad} (min^{-1})	r^2	q_e (mg g^{-1})	h (mg g^{-1} min^{-1})	r^2	k_p (mg g^{-1} min)	r^2	k_t (g mg^{-1} $min^{0.5}$)	$_c$	r^2
0.076	0.90	0.455	0.031	0.93	0.051	0.98	0.046	0.008	0.96

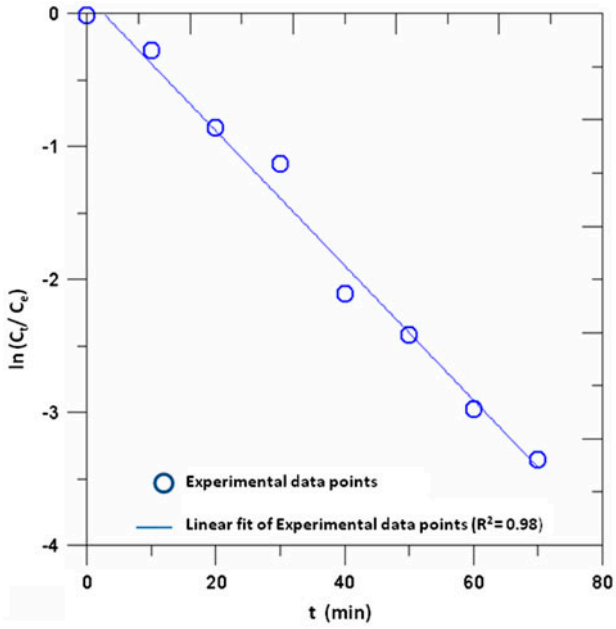

Fig. 7. Plot for interparticle diffusion model (Weber–Morris plots) for arsenic adsorption by IEASA (volume: 500 ml, temperature: 30 ± 2°C, Initial As concentration: 1 mg L^{-1}, adsorbent dose: 2.5 g L^{-1}).

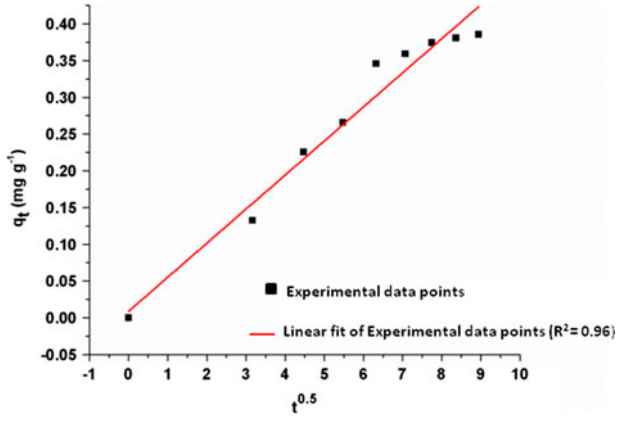

Fig. 8. Plot for intraparticle diffusion model (Weber–Morris plots) for arsenic adsorption by IEASA (volume: 500 ml, temperature: 30 ± 2°C, initial As concentation: 1 mg L^{-1}, adsorbent dose: 2.5 g L^{-1}).

which confirms the superiority and practical applicability of IEASA over other adsorbents.

3.5. Effect of the presence of other co-anions

The presence of various other ions is also reported to significantly affect the arsenate removal efficiency. In order to study the effect of coexisting anions such as sulfate, nitrate, carbonate, bicarbonate, and chloride, which compete in adsorption process, the adsorption studies were carried out in the presence of these anions. TW and SW were spiked with initial concentration of arsenate at 1 mg L^{-1}. The result suggests that there is no significant effect of these coions on arsenate removal efficiency. The arsenate removal efficiency observed for SW and arsenate spiked TW was almost similar confirming that sorption of arsenate on IEASA is not affected by the presence of ions commonly found in TW.

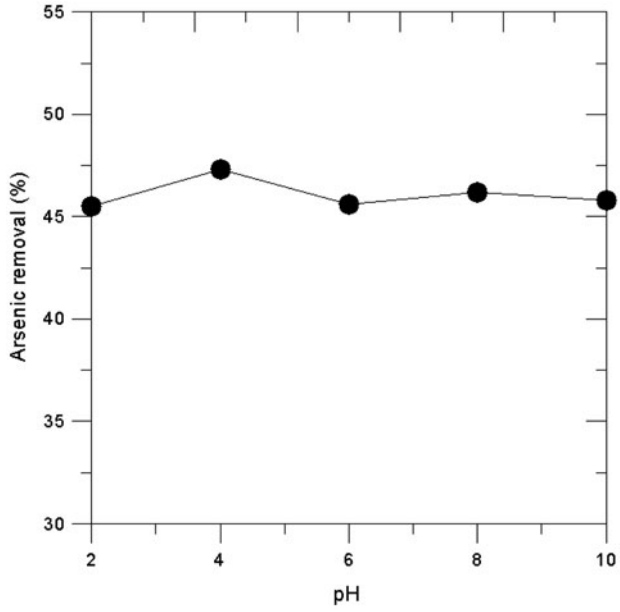

Fig. 9. Effect of pH on arsenic removal by IEASA (batch volume: 100 ml, temperature: 30 ± 2°C, initial As concentation: 1 mg L^{-1}, contact time: 6 h, adsorbent dose: 1.0 g L^{-1}).

3.6. Treated water quality

The use of fly ash-based products for treatment of water is always questionable considering the presence of several toxic elements in fly ash. In order to assess the portability of the treated water and to ascertain whether there is any leaching of such toxic elements from IEASA into the treated water; normal TW used for drinking purpose was spiked with 1 mg L^{-1} of arsenate and was treated with IEASA. Various water quality parameters including concentration of various metals were determined for treated and untreated water and are presented in Table 5. It was found that quality of the water after treatment with IEASA remained almost unaltered, except a slight increase in aluminum concentration and minor changes in pH

Table 5
Physicochemical parameters of water before and after treated with IEASA (volume of water: 100 ml, IEASA dose: 4.0 g l^{-1}, contact time: 24 h)

Parameter	Before adsorption	After adsorption	Desirable limit as per Indian drinking water standard[a]
pH	6.78	7.92	6.5–8.5
Turbidity (NTU)	1.12	1.56	5
Total dissolved solids (mg l^{-1})	223	248	2,000
Alkalinity as $CaCO_3$	96	172	600
Total hardness as $CaCO_3$	120	4	600
Calcium (mg l^{-1})	40.25	1.8	200
Magnesium (mg l^{-1})	0.98	0.21	100
Aluminum (mg l^{-1})	0.01	0.17	0.2
Arsenic (mg l^{-1})	0.96	0.006	0.01
Barium (mg l^{-1})	0.03	BDL	0.7
Copper (mg l^{-1})	0.02	0.01	1.5
Iron (mg l^{-1})	0.15	0.01	0.3
Chromium (mg l^{-1})	BDL	0.01	0.05
Cobalt (mg l^{-1})	BDL	BDL	NA
Manganese (mg l^{-1})	0.01	BDL	0.3
Nickel (mg l^{-1})	BDL	BDL	NA
Lead (mg l^{-1})	BDL	BDL	0.01
Strontium (mg l^{-1})	0.19	0.02	NA
Zinc (mg l^{-1})	0.21	BDL	15

[a]Indian Standard Specifications for Drinking Water (BIS: 10500, 2012).

and alkalinity. Moreover, the concentration of most of the metals were below detection limits in the treated water confirming that these toxic elements present in fly ash have been either removed during the synthesis of IEASA or strongly immobilized in aluminosilicate matrix. The values of various water quality parameters were compared with Indian standard for drinking water (IS: 10500, 2012) and it was found that all the values were below the permissible limits, indicating that the IEASA can be used for treatment of arsenic contaminated drinking water.

4. Proposed mechanism

The presence of cations like iron leads to formation of hydroxide [Fe–OH] groups in aqueous solution that can undergo protonation or deprotonation yielding a surface charge [58,60].

$$Fe–OH + H+ \rightleftharpoons Fe–OH^{2+}$$

$$Fe–OH \rightleftharpoons H^{+} + Fe–O–$$

Anions such as $H_2AsO_4^-$ can be adsorbed through either columbic interaction, according to the following scheme:

$$Fe–OH^{2+} + H_2AsO_4^- \rightleftharpoons Fe–OH^{2+}\ldots–O_4H_2As$$

Or may undergo direct exchange with surface hydroxyl group as shown below:

$$Fe–OH_2^{+} + H_2AsO_4^- \rightleftharpoons Fe—H_2AsO_4 + H_2O$$

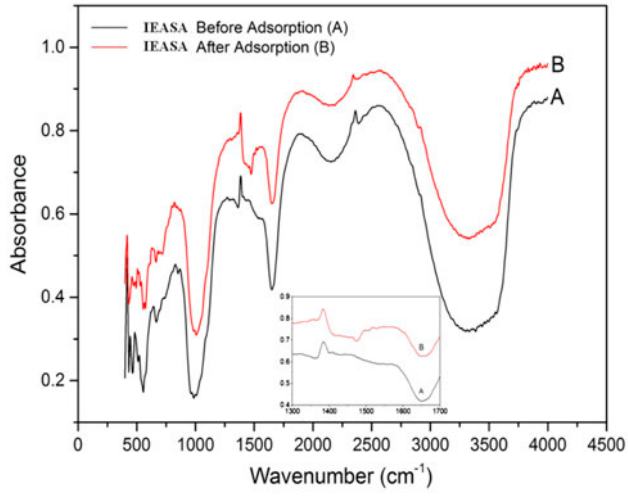

Fig. 10. FTIR spectra of IEASA (before adsorption and after adsorption).

The presence of enhanced surface –OH group in IEASA as compared to CZA is also confirmed by FTIR spectra. The presence of a broad peak at 3,414.98 cm^{-1} suggests the presence Fe–OH complex in IEASA, which was absent in case of CZA (Fig. 2). Further, after adsorption of arsenate, the intensity of this peak has been reduced, indicating the exchange of As with –OH group. An additional peak also appeared at 1,476 cm^{-1} in the saturated adsorbent, which can be assigned to Fe–As complex (Fig. 10).

5. Conclusions

The Faujasite-type IEASA synthesized from fly ash shows excellent removal efficiency for arsenate removal from water. The adsorption efficiency may be attributed to the presence of iron and high Si/Al ratio or Al–OH groups as reactive sites for the adsorption of arsenate anions. The adsorption capacity of the aluminosilicate material was significantly affected by iron content, i.e. Fe-enriched aluminosilicate material exhibited more adsorption efficiency. The material has good efficiency over a wide range of pH and in the presence of other competing co ions. Further, IEASA exhibit fast kinetics which suggests that significantly less time will be required for the treatment of arsenate contaminated water. Studies pertaining to the quality of water after treatment with IEASA, also suggests that the arsenate contaminated water treated with IEASA will be safe for drinking purpose. It can also be concluded from the findings that IEASA can be effectively used in field for arsenic removal for solving the issue of safe drinking water in affected areas.

Acknowledgement

The authors gratefully acknowledge the financial support from CSIR, New Delhi under project ESC0306.

List of the nonstandard abbreviations

- q_e — amount of adsorbate adsorbed per unit weight of adsorbent at equilibrium (mg g^{-1})
- q_m — maximum adsorption capacity (mg g^{-1})
- K_L — Langmuir constant
- Ce — equilibrium concentration of adsorbate in solution (mg L^{-1})
- K_F — Freundlich constant
- q_t — amount of arsenate adsorbed at time t (mg g^{-1})
- k_{ad} — equilibrium rate constant of pseudo-first-order adsorption (min^{-1})
- h — initial sorption rate (mg g^{-1} min^{-1})
- k_p — particle diffusion coefficient (mg g^{-1} min)
- k_i — intraparticle diffusion coefficient (mg g $min^{0.5}$)

References

[1] Arsenic Primer, Guidance for UNICEF Country Offices on the Investigation and mitigation of arsenic contamination, United Nations Children's Fund (UNICEF), New York, NY, 2008.
[2] IARC Monograph on the Evaluation of Carcinogenic Risks to Humans, 100C (2012) 41–85.
[3] Some drinking-water disinfectants and contaminants, including arsenic, IARC Monograph on the Evaluation of Carcinogenic Risks Humans 84 (2004) 41–267.
[4] G. Pershagen, The carcinogenicity of arsenic, Environ. Health Perspect. 40 (1981) 93–100.
[5] A.H. Smith, C. Hopenhayn-Rich, M.N. Bates, H.M. Goeden, I. Hertz-Picciotto, H.M. Duggan, R. Wood, M.J. Kosnett, M.T. Smith, Cancer risks from arsenic in drinking water, Environ. Health Perspect. 97 (1992) 259–267.
[6] A.H. Smith, C.M. Steinmaus, Health effects of arsenic and chromium in drinking water: Recent human findings, Annu. Rev. Public Health 30 (2009) 107–122.
[7] T.S.Y. Choong, T.G. Chuah, Y. Robiah, F.L.G. Koay, I. Azni, Arsenic toxicity, health hazards and removal techniques from water: An overview, Desalination 217 (2007) 139–166.
[8] Drinking water specification (Second revision of IS 10500), Bureau of Indian standards (BIS), 2012.
[9] Guidelines for Drinking Water Quality, fourth ed., World Health Organization (WHO), Geneva, 2011.
[10] European Union (drinking water) regulations, 2014.
[11] National Primary Drinking water Regulations, EPA 816-F-09-0004, United states Environmental protection Agency (USEPA), Washington, DC, 2012.
[12] I. Ali, Z.A. Othman, A. Alwarthan, M. Asim, T. Khan, Removal of arsenic species from water by batch and column operations on bagasse fly ash, Environ. Sci. Pollut. Res. 21 (2014) 3218–3229.
[13] I. Ali, T.A. Khan, M. Asim, Removal of arsenic from water by electrocoagulation and electrodialysis techniques, Sep. Purif. Rev. 40 (2011) 25–42.
[14] I. Ali, V.K. Gupta, T.A. Khan, M. Asim, Removal of arsenic from aqueous solution by electro-coagulation method using Al-Fe electrodes, Int. J. Electrochem. Sci. 7 (2012) 1898–1907.
[15] I. Ali, T.A. Khan, M. Asim, Removal of arsenate from groundwater by electrocoagulation method, Environ. Sci. Pollut. Res. 19 (2012) 1668–1676.
[16] I. Ali, T.A. Khan, I. Hussain, Treatment and remediation methods for arsenic removal from the ground water, Int. J. Environ. Eng. 3 (2011) 48–71.
[17] D. Mohan, C.U. Pittman Jr., Arsenic removal from water/wastewater using adsorbents-A critical review, J. Hazard. Mater. 142 (2007) 1–53.
[18] I. Ali, The quest for active carbon adsorbent substitutes: Inexpensive adsorbents for toxic metal ions removal from wastewater, Sep. Purif. Rev. 39 (2010) 95–171.
[19] I. Ali, New generation adsorbents for water treatment, Chem. Rev. 112 (2012) 5073–5091.
[20] I. Ali, M. Asim, T.A. Khan, Low cost adsorbents for the removal of organic pollutants from wastewater, J. Environ. Manage. 113 (2012) 170–183.

[21] I. Ali, Water TREATMENT by Adsorption columns: Evaluation at ground level, Sep. Purif. Rev. 43 (2014) 175–205.
[22] I. Ali, V.K. Gupta, Advances in water treatment by adsorption technology, Nature 1 (2006) 2661–2667.
[23] R. Menhage-Bena, H. Kazemian, M. Ghazi-Khansari, M. Hosseini, S.J. Shahtaheri, Evaluation of some natural zeolites and their relevant synthetic types as sorbents for removal of arsenic from drinking water, Iran. J. Public Health 33 (2004) 36–44.
[24] G.B. Gholikandi, M.M. Baneshi, E. Dehghanifard, S. Salehi, A.R. Yari, Natural zeolites application as sustainable adsorbent for heavy metals removal from drinking water, Iran. J. Toxicol. 3 (2010) 302–310.
[25] K.B. Vu, M.D. Kaminski, L. Nuñez, Review of Arsenic Removal Technologies for Contaminated Groundwaters, Argonne National Laboratory, Oak Ridge, TN, 2003.
[26] M. Chiban, M.Z. Carja, F.G. Sinan, Application of low-cost adsorbents for arsenic removal: A review, J. Environ. Chem. Ecotoxicol. 4 (2012) 91–102.
[27] D. Bonnin, Arsenic removal from water utilizing natural zeolites, Proceedings Ann. Conf, American Water Works Assoc, Denver, CO, 1997.
[28] Y.H. Xu, T. Nakajima, A. Ohki, Adsorption and removal of arsenic(V) from drinking water by aluminum-loaded Shirasu-zeolite, J. Hazard. Mater. 92 (2002) 275–287.
[29] Y. Xu, A. Ohki, S. Maeda, Removal of arsenate, phosphate, and fluoride ions by aluminium-loaded shirasu-zeolite, Toxicol. Environ. Chem. 76 (2000) 111–124.
[30] J.Q. Jiang, S.M. Ashekuzzaman, A. Jiang, S.M. Sharifuzzaman, S.R. Chowdhury, Arsenic contaminated groundwater and it's treatment options in Bangladesh, Int. J. Environ. Res. Public Health 10 (2013) 18–46.
[31] Z. Li, Combination of co-precipitation with zeolite filtration to remove arsenic from contaminated water, USGS Report, 2011.
[32] D. Bobbin, Method of Removing Arsenic Species from an Aqueous Medium using Modified Zeolite Material, US patent no. US6042731 A, 2000.
[33] A.S. Vakharkar, Adsorption Studies For Arsenic Removal Using Modified Chabazite, Graduate school of thesis and dissertations, University of South Florida, Tampa, FL, 2005.
[34] R.M. Bena, H. Kazemian, S. Shahtaheri, M.G. Khansari, M. Hosseini, Evaluation of iron modified zeolites for removal of arsenic from drinking water, Stud. Surf. Sci. Catal. B 154 (2004) 1892–1899.
[35] C.S. Jeon, S. Park, K. Baek, J.S. Yang, J.G. Park, Application of iron-coated zeolites (ICZ) for mine drainage treatment, Korean J. Chem. Eng. 29 (2012) 1171–1177.
[36] K.B. Payne, T.M.A. Fattah, Adsorption of arsenate and arsenite by iron-treated activated carbon and zeolites: Effects of pH, temperature and ionic strength, J. Environ. Sci. Health, Part A 40 (2005) 723–749.
[37] M.B. Baskan, A. Pala, Batch and fixed batch column studies of arsenic adsorption on natural and modified clinoptilolite, Water Air Soil Poll. 225 (2013) 1798.
[38] Z. Li, J.S. Jean, W.T. Jiang, P.H. Chang, C.J. Chen, L. Liao, Removal of arsenic from water using Fe-exchanged natural zeolite, J. Hazard. Mater. 187 (2011) 318–323.
[39] Z. Li, W.T. Jiang, J.S. Jean, H. Hong, L. Liao, G. Lv, Combination of hydrous iron oxide precipitation with zeolite filtration to remove arsenic from contaminated water, Desalination 280 (2011) 203–207.
[40] M.S. Onyango, Y. Kojima, H. Matsuda, A. Ochieng, Adsorption Kinetics of Arsenic Removal from Groundwater by Iron-Modified Zeolite, J. Chem. Eng. Jpn. 36 (2003) 1516–1522.
[41] L.M. Camacho, R.R. Parra, S. Deng, Arsenic removal from groundwater by MnO2-modified natural clinoptilolite zeolite: Effects of pH and initial feed concentration, J. Hazard. Mater. 189 (2011) 286–293.
[42] S. Shevade, R.G. Ford, Use of synthetic zeolites for arsenate removal from pollutant water, Water Res. 38 (2004) 3197–3204.
[43] Z. Li, R. Beachner, Z. McManama, H. Hanlie, Sorption of arsenic by surfactant-modified zeolite and kaolinite, Microporous Mesoporous Mater. 105 (2007) 291–297.
[44] V. Swarnkar, R. Tomar, Use of Surfactant-Modified Zeolites for Arsenate Removal from Pollutant Water, J. Dispersion Sci. Technol. 33 (2012) 913–918.
[45] E.J. Sullivan, R.S. Bowman, I.A. Legiec, Sorption of arsenic from soil-washing leachate by surfactant-modified zeolite, J. Environ. Qual. 32 (2003) 2378–2391.
[46] A.M. Yusof, N.A. Malek, Removal of Cr(VI) and As (V) from aqueous solutions by HDTMA-modified zeolite Y, J. Hazard. Mater. 162 (2009) 1019–1024.
[47] V. Swarnakar, N. Agrawal, R. Tomar, Sorption of Cr(VI) & As(V) on HDTMA-modified zeolites, Int. J. Sci. Eng. Res. 2 (2011) 163–171.
[48] J. Su, H.G. Huang, X.Y. Jin, X.Q. Lu, Z.L. Chen, Synthesis, characterization and kinetic of a surfactant-modified bentonite used to remove As(III) and As(V) from aqueous solution, J. Hazard. Mater. 185 (2011) 63–70.
[49] J.M. Barrón, A.J. Azuara, R.L. Ramos, M.S.B. Mendoza, R.M.G. Coronado, L.F. Rubio, J.M.M. Rosales, Adsorption of arsenic(V) from a water solution onto a surfactant-modified zeolite, Adsorption 17 (2011) 489–496.
[50] G. McKay, Adsorption of dyestuffs from aqueous solutions with activated carbon I: Equilibrium and batch contact-time studies, J. Chem. Technol. Biotechnol. 32 (2007) 759–772.
[51] H.G. Karge, Fritz-Haber-Institut der Max-Planck-Gesellschaft, Verified Syntheses of Zeolitic Materials Characterization by IR spectroscopy, 2nd Revised Edition, International Zeolite Association, Amsterdam, 2001.
[52] I. Langmuir, The constitution and fundamental properties of solids and liquids. Part I. Solids, J. Am. Chem. Soc. 38 (1916) 2221–2295.
[53] H.M.F. Freundlich, Uber die adsorption in losungen, Z. Phys. Chem. 57A (1906) 385–470.
[54] S. Lagergren, Zur theorie der sogenannten adsorption gelöster stoffe (About the theory of so-called adsorption of soluble substances), Kungliga Svenska Vetenskapsakademiens, Handlingar 24 (1898) 1–39.
[55] Y.S. Ho, G. McKay, Pseudo-second order model for sorption processes, Process Biochem. 34 (1999) 451–465.
[56] W.J. Weber, J.C. Morris, Adsorption Processes for Water Treatment, Buterworth, London, 1987.

[57] M.P.E. Gonz´alez, J. Mattusch, W.D. Einicke, R. Wennrich, Sorption on natural solids for arsenic removal, Chem. Eng. J. 81 (2001) 187–195.
[58] M.P. Elizalde-González, J. Mattusch, R. Wennrich, P. Morgenstern, Uptake of arsenite and arsenate by clinoptilolite-rich tuffs, Microporous Mesoporous Mater. 46 (2001) 277–286.
[59] M. Benjamin, R.S. Sletten, R.P. Bailey, T. Bennett, Sorption and filtration of metals using iron oxide coated sand, Water Res. 30 (1996) 2609–2620.
[60] A. Carrillo, J.I. Drever, Adsorption of arsenic by natural aquifer material in the San Antonio-El Triunfo mining area, Baja California, Mexico, Environ. Geol. 35 (1998) 251–257.